Am J Physiol Endocrinol Metab 305: E1495–E1511, 2013.
First published October 29, 2013; doi:10.1152/ajpendo.00366.2013.

Divergent compensatory responses to high-fat diet between C57BL6/J and C57BLKS/J inbred mouse strains

Emily K. Sims,[1] Masayuki Hatanaka,[1,5] David L. Morris,[2] Sarah A. Tersey,[1,5] Tatsuyoshi Kono,[2] Zunaira Z. Chaudry,[2] Kathleen H. Day,[2] Dan R. Moss,[2] Natalie D. Stull,[1,5] Raghavendra G. Mirmira,[1,2,3,4,5] and Carmella Evans-Molina[2,3,4,5]

[1]*Department of Pediatrics, Indiana University School of Medicine, Indianapolis, Indiana;* [2]*Department of Medicine, Indiana University School of Medicine, Indianapolis, Indiana;* [3]*Department of Cellular and Integrative Physiology, Indiana University School of Medicine, Indianapolis, Indiana;* [4]*Department of Biochemistry and Molecular Biology, Indiana University School of Medicine, Indianapolis, Indiana; and* [5]*The Herman B Wells Center for Pediatric Research, Indiana University School of Medicine, Indianapolis, Indiana*

Submitted 1 July 2013; accepted in final form 24 October 2013

Sims EK, Hatanaka M, Morris DL, Tersey SA, Kono T, Chaudry ZZ, Day KH, Moss DR, Stull ND, Mirmira RG, Evans-Molina C. Divergent compensatory responses to high-fat diet between C57BL6/J and C57BLKS/J inbred mouse strains. *Am J Physiol Endocrinol Metab* 305: E1495–E1511, 2013. First published October 29, 2013; doi:10.1152/ajpendo.00366.2013.—Impaired glucose tolerance (IGT) and type 2 diabetes (T2DM) are polygenic disorders with complex pathophysiologies; recapitulating them with mouse models is challenging. Despite 70% genetic homology, C57BL/6J (BL6) and C57BLKS/J (BLKS) inbred mouse strains differ in response to diet- and genetic-induced obesity. We hypothesized these differences would yield insight into IGT and T2DM susceptibility and response to pharmacological therapies. To this end, male 8-wk-old BL6 and BLKS mice were fed normal chow (18% kcal from fat), high-fat diet (HFD; 42% kcal from fat), or HFD supplemented with the PPARγ agonist pioglitazone (PIO; 140 mg PIO/kg diet) for 16 wk. Assessments of body composition, glucose homeostasis, insulin production, and energy metabolism, as well as histological analyses of pancreata were undertaken. BL6 mice gained weight and adiposity in response to HFD, leading to peripheral insulin resistance that was met with increased β-cell proliferation and insulin production. By contrast, BLKS mice responded to HFD by restricting food intake and increasing activity. These behavioral responses limited weight gain and protected against HFD-induced glucose intolerance, which in this strain was primarily due to β-cell dysfunction. PIO treatment did not affect HFD-induced weight gain in BL6 mice, and decreased visceral fat mass, whereas in BLKS mice PIO increased total fat mass without improving visceral fat mass. Differences in these responses to HFD and effects of PIO reflect divergent human responses to a Western lifestyle and underscore the careful consideration needed when choosing mouse models of diet-induced obesity and diabetes treatment.

C57BL/6J; C57BLKS/J; diet-induced obesity; pioglitazone; mouse models of T2DM

GENOMEWIDE ASSOCIATION STUDIES (GWAS) indicate that the vast majority of impaired glucose tolerance (IGT) and type 2 diabetes mellitus (T2DM) are polygenic and represent a complex interplay between genetic susceptibility, dietary and lifestyle choices, and environment (48). The initial treatment of T2DM typically consists of a combination of antihyperglycemic agents, including metformin, sulfonylureas, PPARγ agonists, or thiazolidinediones (TZDs), and incretin-based therapies; however, this approach is associated with high secondary failure rates, and many patients will ultimately transition to insulin therapy in order to achieve glycemic targets (45). While the field of T2DM pharmacogenomics is relatively undeveloped compared with other complex diseases, large clinical studies have revealed important differences in response to these therapies based on sex, ethnicity, and other genetic differences (9, 51). Given the heterogeneous nature of IGT and T2DM susceptibility and treatment response, modeling these disorders in the laboratory setting using inbred strains of mice is fraught with inherent challenges.

C57BL/6J (BL6) mice are one of the most widely utilized inbred strains in biomedical research (1). Many knockout and transgenic mouse models are bred congenic on the BL6 background for metabolic analysis, and BL6 mice are typically selected to model diet-induced obesity (5, 7, 32, 40). The C57BLKS/J (BLKS) strain inadvertently arose from the BL6 background as a result of genetic contamination. Subsequent analysis of the BLKS genome demonstrated ~70% contribution from the BL6 mouse, with 20% from the DBA/2J mouse and 9% from an unidentified source (8, 29). In contrast to the BL6 strain, BLKS mice have been characterized as relatively more resistant to diet-induced obesity (39). Interestingly, in the context of severe insulin resistance conferred by functional leptin deficiency, BL6 and BLKS mice both initially develop hyperglycemia (18). However, BL6 mice are able to compensate with increased insulin production, ultimately developing only glucose intolerance. In contrast, the BLKS strain develops severe and progressive hyperglycemia with islet atrophy (18). The mechanistic reasons for these divergent phenotypes are incompletely understood.

We hypothesized that distinct phenotypic responses to diet-induced obesity between the BL6 and BLKS parent strains would yield important insights into variations in diabetes susceptibility and disease risk. Because clinical trials utilizing agonists of the nuclear hormone receptor peroxisome proliferator-activated receptor-γ (PPARγ) for diabetes prevention and treatment have identified "responders" and "nonresponders", we also sought to analyze differences in response to the TZD drug pioglitazone initiated concurrently with high-fat diet (HFD) treatment. To this end, male BL6 and BLKS mice were fed either normal chow containing 18% of calories from fat, HFD comprised of 42% of calories from fat to simulate the typical Western diet, or HFD supplemented with the PPARγ agonist pioglitazone (HFD+PIO), for up to 16 wk. Body composition, glucose

Address for reprint requests and other correspondence: C. Evans Molina, Indiana Univ. School of Medicine, 635 Barnhill Dr., MS 2031A, Indianapolis, Indiana 46202 (e-mail: cevansmo@iu.edu).

metabolism, β-cell function, death, and architecture, and energy metabolism were analyzed. Our results demonstrate that underlying genetic differences as well as behavioral responses between these strains translate into important and divergent physiological responses to overnutrition and PPARγ agonist therapy. Differences observed between the BL6 and BLKS strains may reflect divergent responses of humans to a Western lifestyle and pharmacological therapy and underscore the careful consideration needed when choosing mouse models of diet-induced obesity and T2DM treatment and when broadly extrapolating preclinical results from one inbred rodent strain to heterogeneous human populations.

MATERIALS AND METHODS

Animals and metabolic testing. Male BL6 and BLKS mice were obtained from Jackson Laboratories (Bar Harbor, ME) and maintained under protocols approved by the Indiana University School of Medicine Institutional Animal Care and Use Committee in accord with the Association for Assessment and Accreditation of Laboratory Animal Care guidelines. Beginning at 8 wk of age, animals were fed either normal chow (Harlan-Teklad Global, catalog number 2018S) containing 18% calories from fat (regular diet), high-fat diet (Harlan-Teklad Global, catalog no. TD88137) containing 42% calories from fat (HFD), or high-fat diet compounded by Harlan-Teklad Global with 140 mg/kg pioglitazone (HFD+PIO). This ratio of drug to chow was calculated to provide a dose of 20 $mg \cdot kg^{-1} \cdot day^{-1}$ PIO. All mice were kept on a standard light-dark cycle with ad libitum access to chow and water. Animals were housed five mice per cage, and food was changed and measured twice weekly. Analyses were performed by the same group of three individuals on three separate cohorts of mice.

Intraperitoneal glucose tolerance tests (IPGTTs) were performed after 10 wk on diet following a 16-h fast and intraperitoneal injection of 2 g/kg D-glucose solution. Blood was sampled from the tail vein at 0, 10, 20, 30, 60, 90, and 120 min, and glucose was measured using a glucometer (AlphaTRAK, Abbott Park, IL). Intraperitoneal insulin tolerance tests (IPITTs) were performed on random fed mice following an intraperitoneal injection of 0.75 U/kg Humulin-R insulin (Lilly, Indianapolis, IN). Blood glucose was measured from tail vein blood at 0, 15, 30, 45, and 60 min. Fasting serum insulin was measured using an ultrasensitive mouse insulin ELISA (Crystal Chem, Downers Grove, IL). The homeostasis model of assessment of insulin resistance (HOMA-IR) was calculated as fasting glucose (mM) × fasting insulin (μU/ml)/22.5 (46).

Body composition was measured by dual-energy X-ray absorptiometry (DEXA) after 12 wk of diet, using a Lunar PIXIMus DEXA Scanner (GE Medical Systems, Fairfield, CT) on mice anesthetized with inhaled isofluorane. Indirect calorimetry measures were performed after 12 wk of diet using a TSE systems LabMaster Metabolism Research Platform (Chesterfield, MO) equipped with calorimeter, feeding, and activity system. All measurements were performed after a 24-h acclimation period followed by 24 h of data collected every 10 min. Respiratory quotient (RQ) and energy expenditure (EE) were calculated as previously described (44), and results are displayed in terms of mean measurements over a 24-h period as well as during light (0700–1900) and dark cycles (1900–0700). Percent relative cumulative frequency (PRCF) curves were generated from RQ values as previously described (33).

For 10 animals per group, euthanized after 14–15 wk on diet, blood was obtained by cardiac puncture on random fed mice for measurement of serum insulin and leptin levels, which were assessed using ELISA assays (Crystal Chem, Downers Grove, IL). To provide an in vivo measurement of β-cell death, multiplex PCR analysis of differentially methylated insulin DNA was performed on terminal serum collected from five animals per group after 12–13 wk of diet, as previously described (12).

Epididymal fat was isolated, frozen in liquid nitrogen, and stored at −80°C until analysis. Total RNA was isolated using RNeasy Lipid Tissue Kit (Qiagen, Valencia, CA) according to the manufacturer's instructions, and the optional on-column DNase digestion step was performed for each sample. cDNA was generated from 1.0 μg of total RNA using M-MLV Reverse Transcriptase and random hexamers (both from Invitrogen, Life Technologies, Grand Island, NY). qRT-PCR was performed using SYBR Green (Sigma-Aldrich, St. Louis, MO) and data were collected using a Mastercycler ep realplex instrument (Eppendorf, Hauppage, NY). PCR primers used for qRT-PCR were: leptin (forward: 5′-GAGACCCCTGTGTCGGTTC-3′; reverse: 5′-CTGCGTGTGAAATGTCATTG-3′), adiponectin (forward: 5′-CAGTGGTCTAGGACCCGAGAA-3′; reverse: 5′-AGGGGGAGATGTTCAGCATGT-3′), and acidic ribosomal phosphoprotein (Arbp; forward: 5′-GCAGGCATCCCAGGACATC-3′; reverse: 5′-GCGATACATATAAGCGGCTTCT-3′). Arbp expression was used as the internal control for data normalization. Samples were assayed in triplicate and relative expression was determined using the $2^{-\Delta\Delta C_T}$ method.

Immunofluorescence and morphometric analysis. Pancreata from at least five mice per treatment group were fixed by cardiac perfusion with 4% paraformaldehyde, paraffin embedded, and sectioned longitudinally at 5-μm intervals. Immunohistochemical analysis of insulin (rabbit anti-human insulin, Santa Cruz, 1:500) was performed as previously described (14). Immunofluorescence experiments were performed for insulin (guinea pig anti-porcine, Invitrogen, 1:250), glucagon (rabbit anti-mouse, Santa Cruz, 1:500), phosphohistone H3 (PH3; rabbit anti-mouse, Millipore, 1:150), and nuclei (diamidino-2-phylindole, DAPI). Secondary antibodies were goat anti-rabbit antibody conjugated to Alexa fluor 488 (Molecular Probes, 1:50) and goat anti-guinea pig antibody conjugated to Alexa fluor 555 (Molecular Probes, 1:200). A Zeiss Axio Observer Z1 inverted microscope equipped with an Orca ER CCD camera (Hamamatsu Photonics, Hamamatsu City, Japan) was used to acquire digital images of the entire stained longitudinal pancreatic section. The β-cell area of five sections, each separated by at least 60 μm, from at least five animals in each group, was calculated using Axio-Vision Software (Zeiss, Thornwood, NY).

To assess proliferation, four pancreatic sections, each separated by at least 100 μm, from at least three mice per group, were immunostained for insulin, PH3, and DAPI, and cells that stained positive for insulin, PH3, and DAPI were counted using Image J software (36). Total insulin-positive cells (positive for insulin and DAPI) counted per animal ranged from 1,961 to 10,565; (mean of 5,110 ± 600 SE). Results were expressed as the percentage of cells positive for all three stains relative to the total number of insulin-positive cells (2).

Glucose-stimulated insulin secretion. Mouse islets were isolated from collagenase-perfused pancreata (CIzyme MA; VitaCyte, Indianapolis, IN) and neutral protease (CIzyme BP Protease, VitaCyte) as previously described (38). Glucose-stimulated insulin secretion (GSIS) was performed as previously described, using ~40 islets per mouse (15). Briefly, islets were preincubated in SAB buffer with 2.5 mM glucose for 1 h, switched to SAB buffer containing 2.5 mM glucose for an additional hour, and then 15 mM glucose for another hour. Supernatants were collected and assayed using a radioimmunometric assay for insulin (Siemens Healthcare Diagnostics, Deerfield, IL); values were normalized to total protein content of the islet fraction.

Islet microarray. After 12 wk of diet, islets from four mice per group were shipped to Miltenyi Biotec (Auburn, CA) on dry ice, where RNA was isolated and Agilent Whole Mouse Genome Oligo Microarray was performed (MACS molecular, Miltenyi Biotec, Auburn, CA). Differential gene expression candidates were considered significant if the P value after one-way analysis of variance (with Tukey posttest) was <0.05 and average expression between groups was at least 1.5-fold different. Differentially expressed reporters were

hierarchically clustered (Euclidean distance, complete linkage). The data discussed in this publication have been deposited in NCBI's Gene Expression Omnibus and are accessible through GEO Series accession no. GSE51055 (http://www.ncbi.nlm.nih.gov/geo/query/acc.cgi?acc=GSE51055) (11). (It is also linked to the online version of this paper.)

Statistical analysis. Data values are presented as means ± SE. One-way analysis of variance (with Tukey posttest) was used for comparison of results within and between strains. Multiplicity adjusted *P* values were calculated to account for multiple comparisons. A *P* value of <0.05 was taken to indicate the presence of a significant difference. Prism 6 software (GraphPad, La Jolla, CA) was used for all statistical analyses, with the exception of those performed by Miltenyi Bioinformatics in the evaluation of microarray results.

RESULTS

BL6 mice gain more weight and visceral adiposity on HFD than BLKS mice; PIO decreased visceral adiposity in BL6 mice and increased total adiposity in BLKS mice. To assess changes in body composition over time in response to dietary and pharmacologic intervention, mice were weighed weekly, and DEXA scans were obtained after 12 wk on diet. No significant differences existed in body weight or the percentage of total or visceral fat between strains on regular diet (Fig. 1, *E, K, N*). In both strains, weight gain was increased with HFD (Fig. 1, *A–E*); however, BL6 mice gained significantly more weight on HFD than BLKS mice (Fig. 1*E*). In BLKS mice, the addition of PIO increased weight gain compared with HFD alone, but this effect was notably absent in the BL6 strain (Fig. 1, *A–E*). Lean mass did not differ within strains, but BL6 mice had significantly greater lean mass compared with each respective BLKS comparison group (data not shown).

While BL6 mice accumulated significantly more total fat mass than BLKS mice fed HFD (Fig. 1*H*), both strains demonstrated similarly increased percentages of body fat with HFD treatment compared with the regular diet group (Fig. 1, *I–K*). The addition of PIO had differing effects in each strain. In BL6 mice on HFD+PIO, fat mass was unchanged compared with HFD alone (Fig. 1, *F, I*). In contrast, compared with the HFD group, BLKS mice on HFD+PIO had an increase in total fat mass, although the percentage of body fat was not significantly different (Fig. 1, *G, J*).

Epididymal white adipose tissue (eWAT) was dissected, weighed, and expressed as a percentage of total body weight in order to estimate changes in visceral fat content (Fig. 1, *L–N*). HFD treatment significantly increased visceral adiposity in both strains, but comparison between strains revealed that BL6 mice on HFD had significantly more eWAT as a percentage of body weight than BLKS mice on HFD. Interestingly, the addition of PIO decreased visceral adiposity in BL6 mice, whereas this effect was notably absent in BLKS mice. These data indicate that, compared with BLKS mice, BL6 mice demonstrated increased body weight accumulation and increased ability to expand the visceral fat depot in response to HFD. BL6 mice were also more responsive to the effects of PIO to decrease visceral adiposity.

HFD worsens glucose tolerance in both strains. To assess changes in glucose tolerance, IPGTTs were performed after 10 wk of dietary intervention. On regular diet, BL6 mice tended to be less glucose tolerant than their BLKS counterparts ($P = 0.08$). HFD worsened glucose tolerance in both the BL6 and BLKS strains (Fig. 2, *A–D*). The addition of PIO significantly improved glucose tolerance in HFD-fed BL6 mice. The area under the curve analysis of the IPGTT for BLKS mice on HFD+PIO was likewise indistinguishable from that of BLKS mice fed regular diet. Between-strain differences are shown in Fig. 2*E*. Compared with BL6 mice, BLKS mice demonstrated significantly better glucose tolerance following HFD treatment.

BL6 mice have increased insulin resistance irrespective of diet compared with BLKS mice, and increased insulin production on HFD. To determine whether differences in insulin resistance contributed to changes in glucose tolerance, IPITTs were also performed 10 wk after dietary intervention. Although differences between diet groups were not significant within strains, comparison between strains revealed that BLKS mice were more insulin sensitive than corresponding BL6 mice (Fig. 3, *A–E*). HOMA-IR calculations were performed as a surrogate measurement of insulin resistance, and comparison between strains revealed that HOMA-IR was significantly increased in BL6 mice on HFD but remained stable in BLKS mice across the three treatment groups (Fig. 3, *L–N*).

Fasting and fed serum insulin levels were measured to provide a context for changes in glucose and insulin tolerance. Serum insulin levels were markedly increased in BL6 mice on HFD, and this effect was largely normalized by PIO (Fig. 3, *F, I*). Interestingly, despite a worsening of glucose tolerance in BLKS mice, no significant differences in serum insulin levels were noted in any of the BLKS treatment groups (Fig. 3, *G, J*). Compared with the BLKS strain, BL6 mice demonstrated significant hyperinsulinemia in response to HFD challenge (Fig. 3, *H, K*). Together, these data indicate that BL6 mice were able to increase insulin levels in response to HFD. In contrast, compensatory hyperinsulinemia was absent in the BLKS strain. PIO normalized insulin levels in BL6 mice, with no apparent effect in BLKS mice.

HFD results in altered adipose-derived hormone expression in BL6 mice. Because HFD significantly increased visceral fat mass in both strains, we next sought to compare changes in gene expression within the epididymal fat depot. Quantitative RT-PCR was performed on epididymal adipose tissue to evaluate the relative mRNA expression levels of adiponectin and leptin. In BL6 mice, adiponectin expression was significantly decreased in mice on HFD, and this was normalized by the addition of PIO (Fig. 4*A*). Interestingly, no significant difference in adiponectin expression was noted among the BLKS groups (Fig. 4*B*). A threefold increase in leptin expression was observed in the epididymal fat of BL6 mice on HFD, whereas leptin expression in BL6 mice on HFD+PIO was not significantly different compared with mice on regular or HFD diet (Fig. 4*D*). In contrast, BLKS mice demonstrated no change in epididymal adipose leptin expression between any treatment group (Fig. 4*E*). Comparisons between strains revealed that BL6 mice fed HFD had significantly higher leptin expression than BLKS mice (Fig. 4*F*). Serum leptin levels were also measured by ELISA after 15 wk of dietary intervention, and, strikingly, similar patterns were noted. BL6 mice fed HFD exhibited a dramatic 20-fold increase in serum leptin compared with regular diet treatment. PIO significantly decreased this response, but levels were still higher than those found under regular diet conditions (Fig. 4*G*). Interestingly, no significant differences in serum leptin were noted between any of the

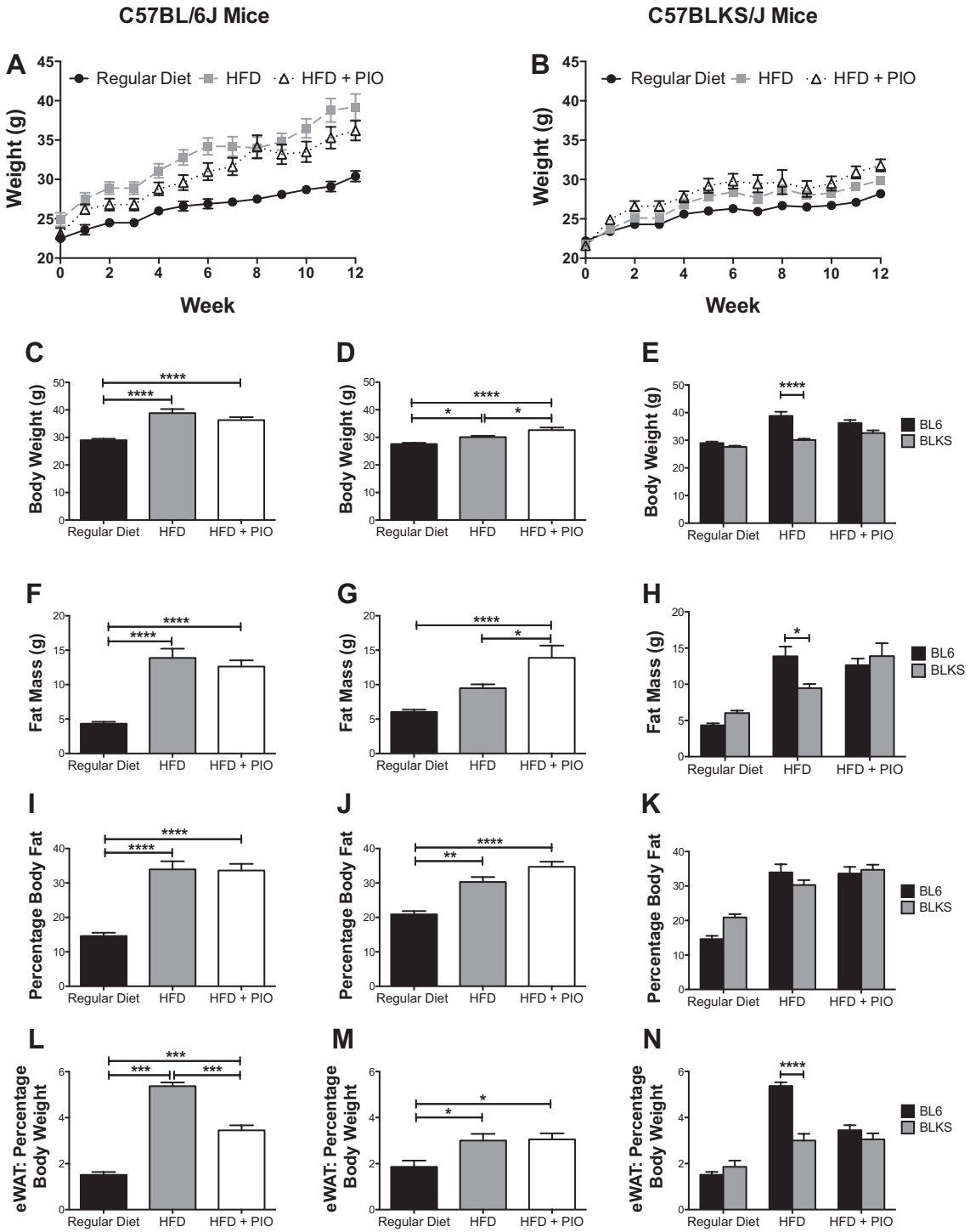

Fig. 1. High-fat diet (HFD) results in greater weight gain and visceral adiposity, whereas pioglitazone (PIO) improves visceral adiposity in BL6 mice. *A* and *B*: weight gain in C57BL6/J (BL6) and C57BLKS/J (BLKS) mice fed chow containing 18% calories from fat (Regular Diet), HFD (containing 42% calories from fat), or HFD+PIO was measured weekly over a 12-wk period. *C–E*: body weights after 12 wk on study diet. *F–H*: DEXA measurements were performed after 12 wk on study diets to measure fat mass; $n = 10–13$ mice per treatment group. *I–K*: %body fat was calculated based on measured fat mass as %body weight; $n = 10–13$ mice per treatment group. *L–N*: visceral fat mass was measured by epididymal white adipose tissue dissection, which was weighed and expressed as %total body weight after 16 wk on study diets; $n = 7–10$ per group. Results are displayed as means ± SE. $^{*}P < 0.05$, $^{**}P < 0.01$, $^{***}P < 0.001$, $^{****}P < 0.0001$ for indicated comparisons.

BLKS groups (Fig. 4*H*). Comparisons between strains revealed that both BL6 mice on HFD and HFD+PIO had significantly higher serum leptin levels than the BLKS mice in the same treatment groups (Fig. 4*I*). In aggregate, these data suggest that increased total and visceral fat accumulation seen in BL6 mice on HFD was accompanied by decreased visceral fat adiponectin expression and increased leptin expression and marked hyperleptinemia. Changes in visceral fat accumulation with

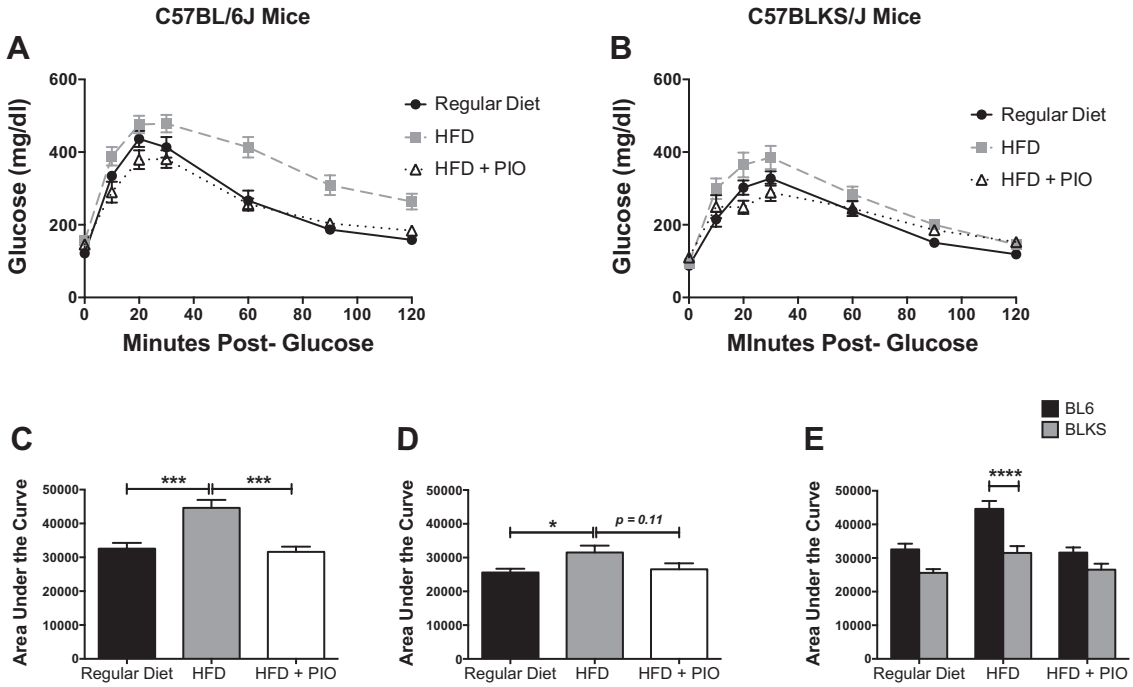

Fig. 2. HFD worsens glucose tolerance in BL6 to a greater degree than BLKS mice, whereas PIO restores glucose tolerance in HFD-treated mice. *A* and *B*: BL6 and BLKS mice fed Regular Diet, HFD, or HFD+PIO for 10 wk were fasted overnight and injected intraperitoneally with 2 g/kg glucose. Blood glucose concentration was measured over the course of 2 h. *C–E*: corresponding area under curve (AUC) analyses for intraperitoneal glucose tolerance tests; $n = 10$ per group. Results are displayed as means ± SE. $^{*}P < 0.05$, $^{**}P < 0.01$, $^{***}P < 0.001$, $^{****}P < 0.0001$ for indicated comparisons.

PIO were correlated with either complete or relative normalization of adiponectin and leptin expression in BL6 mice. Interestingly, despite increased visceral fat accumulation with HFD, changes in adiponectin and leptin expression were largely absent in BLKS mice.

BL6 mice demonstrate increased β-cell area percentage in response to HFD, whereas BLKS mice on HFD demonstrate increased β-cell death. Given the worsening in glucose tolerance but divergent findings with regard to serum insulin levels, we next sought to define changes in β-cell function and architecture. To assess changes in islet morphometry after dietary intervention, pancreata were removed after 14 wk of treatment and stained for insulin and glucagon. There was no change in the expected murine islet architecture with HFD or HFD+PIO treatment in either strain (Fig. 5, *A, B*). The β-cell area percentage (relative to total pancreas area) was significantly increased in BL6 mice on HFD (Fig. 5, *C–E*), whereas β-cell area percentage in animals on HFD+PIO was not statistically different compared with mice on regular diet. Similar to serum insulin levels, no statistical difference in β-cell area percentage was noted between the BLKS groups (Fig. 5*D*).

β-Cell proliferation was assessed by costaining pancreata for insulin and PH3, which marks cells in the G2 and M phases of mitosis (20). Consistent with the analysis of β-cell area percentage, BL6 mice on HFD had increased insulin- and PH3-positive cells, although the significance of this effect was limited by variability (Fig. 5*F*). In contrast, PH3-positive β-cells tended to decrease in BLKS mice on HFD ($P = 0.099$), with significantly fewer cells in BLKS mice on HFD+PIO compared with regular diet ($P < 0.01$; Fig. 5*G*). Between-strain comparisons yielded no differences in β-cell area percentage or proliferation (Fig. 5, *E*, *H*).

Differential methylation of circulating preproinsulin DNA was measured to assess β-cell death. No differences existed between BL6 groups on different diets (Fig. 5*I*). However, BLKS mice on HFD demonstrated a marked increase in the serum unmethylation index, reflecting increased β-cell death. This finding was partially reversed by the addition of PIO (Fig. 5*J*). BLKS mice on HFD had a significantly higher proportion of circulating unmethylated DNA compared with BL6 mice on HFD (Fig. 5*K*).

To assess differences in islet function ex vivo, islets were isolated and allowed to recover overnight, and GSIS assays were performed (Fig. 5*L*). As previously reported, under regular diet conditions, BLKS islets displayed a more robust response to high glucose compared with BL6 islets (3). However, there was a progressive decrease in GSIS of islets from BLKS mice fed HFD that reached statistical significance in the HFD+PIO group. This effect of HFD on islet function was absent among BL6 treatment groups. These findings are suggestive of HFD induced β-cell dysfunction in BLKS mice.

Islet gene expression is differentially regulated in BL6 and BLKS mice on HFD and in response to PIO. Microarray using whole islet RNA was performed after 12 wk of dietary intervention. Normalization and correlation analysis of the data revealed only minor variability between replicate experiments and did not identify any clear outliers within groups. Differential gene expression analysis (displayed in Figs. 6 and 7, using heat maps and Venn diagrams) revealed 99 genes with increased expression in islets of BL6 mice on HFD compared with regular chow that were not increased in islets of BLKS mice fed HFD (Fig. 6*C*) and 169 genes that were uniquely decreased in the BL6 strain by HFD (Fig. 7*C*). BLKS mice also

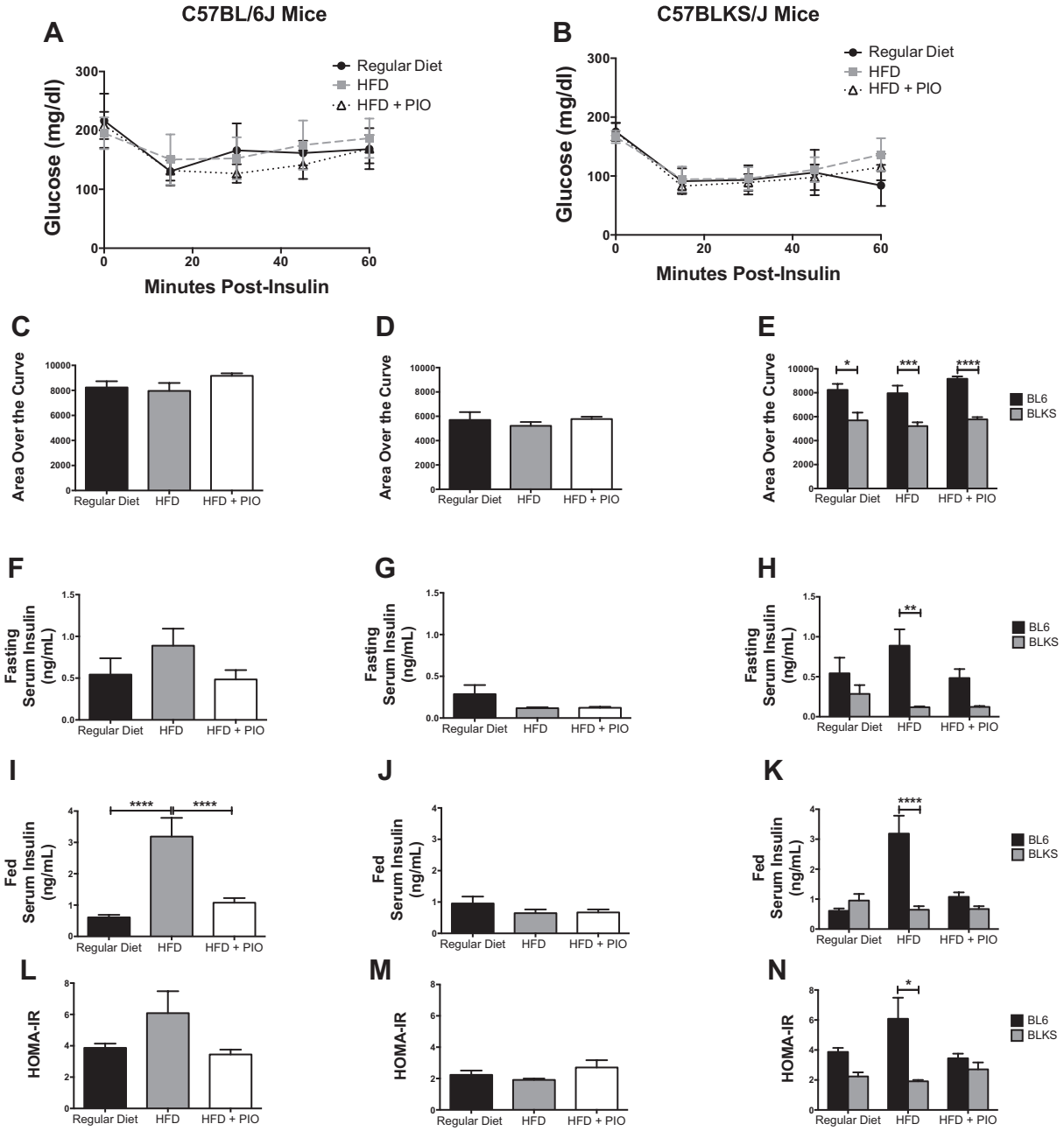

Fig. 3. Serum insulin levels are increased in BL6 mice on HFD but unchanged between diet groups in BLKS mice. *A* and *B*: random-fed BL6 and BLKS mice treated with Regular Diet, HFD, or HFD+PIO for 10 wk were injected intraperitoneally with 0.75 U/kg insulin, and blood glucose concentrations were measured over the course of 60 min. *C–E*: AUC analysis was performed. *F–H*: fasting serum was collected after 11 wk on diet, and insulin levels were quantitated using ELISA; $n = 5$ mice per treatment group. *I–K*: random-fed serum was collected after 16 wk on diet, and insulin levels were quantitated using ELISA; $n = 10$ mice per treatment group. *L–N*: HOMA-IR scores were calculated as described in MATERIALS AND METHODS after 11 wk on study diets; $n = 3$ mice per group. Results for *C–N* are displayed as means ± SE. $^*P < 0.05$, $^{**}P < 0.01$, $^{***}P < 0.001$, $^{****}P < 0.0001$ for indicated comparisons.

had distinct changes in islet gene expression induced by HFD, with 146 genes showing a pattern of increased expression that was absent in BL6+HFD islets (Fig. 6*C*), whereas 161 genes uniquely decreased by HFD in BLKS mice (Fig. 7*C*). Interestingly only one gene was identified that was increased in HFD in both strains; the identity of this gene was unknown. Similarly, only one common gene was decreased in both strains, and the function of this gene was unknown (*Mus musculus* predicted gene 2,569).

Addition of PIO to HFD also had differential effects on islet gene expression between strains. Of 100 genes increased by treating BL6 mice with HFD, 31 (31%) were reversed by treatment with PIO (Fig. 6*D*) and 33 of 170 (19.4%) genes that were decreased by treating BL6 mice with HFD were reversed by treatment with PIO (Fig. 7*D*). BLKS islets demonstrated less response to PIO at the level of gene expression, with reversal of gene expression in 26 of 150 (17.3%) genes increased by HFD (Fig. 6*E*) and reversal of expression in only 8

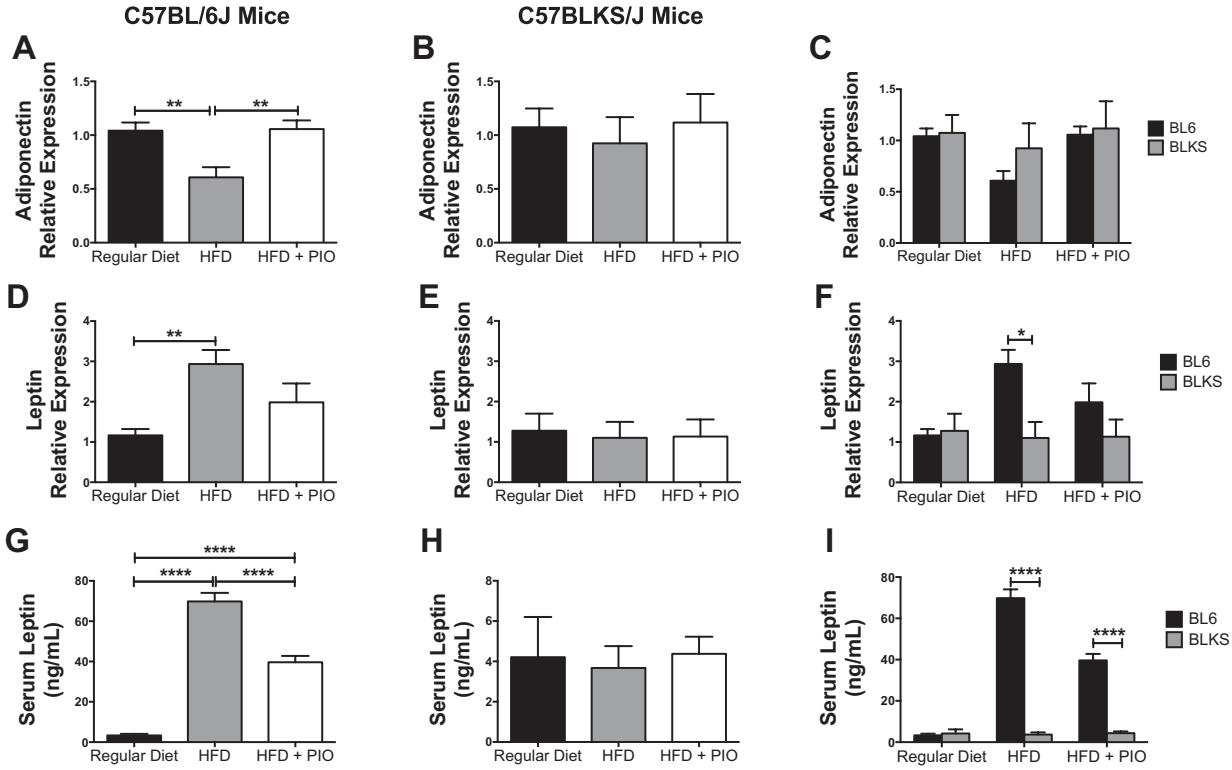

Fig. 4. Changes in adiponectin and leptin expression and serum leptin levels were more pronounced in BL6 mice fed HFD and partially normalized with PIO. Adiponectin (*A–C*) and leptin gene expression (*D–F*) were measured in epididymal white adipose tissue by qRT-PCR in BL6 and BLKS mice fed regular Diet, HFD, or HFD+PIO for 16 wk. *G–I*: random-fed serum was collected after 16 wk on diet, and leptin levels were quantitated using ELISA; n = 7–10 mice per treatment group. Results are displayed as means ± SE. $^{*}P < 0.05$, $^{**}P < 0.01$, $^{***}P < 0.001$, $^{****}P < 0.0001$ for indicated comparisons.

of 162 (4.9%) of genes that were decreased by treatment with HFD (Fig. 7*E*).

Important between-strain differences were noted in pathways identified as important for β-cell function and adaptation, including genes encoding for proteins that regulate growth, proliferation, and inflammation. Table 1 summarizes notable genes that were differentially regulated by HFD in each category, and reversal of HFD-induced changes with PIO treatment are indicated (Table 1). A seminal report from the Attie group (21) has previously compared gene expression patterns in islet of diabetes-resistant BL6 and diabetes-susceptible BTBR strains with *ob/ob* mutations. Genes in our study that were noted to have similar patterns of expression compared with the Attie study are also indicated in Table 1.

BLKS mice show maintained kilocalorie intake on HFD. Metabolic cages were utilized to measure differences in food intake between each strain. Intake in grams was monitored over a 24-h period, and this information was used to calculate kilocalorie intake. Animals on a regular diet demonstrated a clear peak of nocturnal intake. Interestingly, both strains on HFD tended to eat more consistently throughout the monitoring period (Fig. 8, *A, B*). Monitoring revealed no differences in grams of food consumed by BL6 mice on different diets (Fig. 8*C*). In contrast, BLKS mice on HFD ate significantly fewer grams of food compared with BLKS mice on regular chow (Fig. 6*D*). In terms of caloric intake, these differences translated to a significant increase in kilocalories consumed by BL6 mice on HFD and HFD+PIO (Fig. 8*E*). In contrast, kilocalorie consumption was stable in BLKS mice fed regular diet or HFD (Fig. 8*F*).

BLKS mice demonstrate increased activity on HFD. Indirect calorimetry was used to analyze differences in activity by recording the number of beam breaks occurring in the $x+y$- and z-axes. As shown in Fig. 9, *A–C*, measurements differed between strains and within groups. Compared with regular diet, the average number of beam breaks was significantly decreased in BL6 mice on HFD. The addition of PIO to HFD partially restored activity to the level observed in the regular chow group (Fig. 9*A*). These patterns persisted through both light and dark cycles of the 24-h monitoring period (Fig. 9, *D, G*). Conversely, BLKS mice on HFD demonstrated a significant increase in movement counts throughout the 24-h period (Fig. 9*B*). BLKS mice on HFD+PIO also had increased activity during the dark cycle compared with mice on regular chow (Fig. 9*H*), but the differences were not significant during the light cycle (Fig. 9*E*). Strikingly, comparison between strains revealed that BL6 mice demonstrated increased beam breaks recorded compared with BLKS mice under regular diet conditions. However, a complete reversal of this pattern was noted with HFD, where BLKS mice manifested significantly increased activity compared with the BL6 mice fed HFD (Fig. 9, *C, F, I*).

BLKS mice demonstrate increased RQ values. RQ values were calculated to provide insight regarding fuel utilization. As expected, RQ values were significantly decreased over the entire time period for both strains on HFD compared with regular diet, and this difference was most pronounced during the dark cycle (Figs. 7, *A*, *B*, and 10, *A*, *B*). The addition of PIO to HFD increased the RQ during the dark cycle for BL6 mice and increased the RQ during the light cycle for BLKS mice (Fig. 10, *F*, *D*). Differences between strains were most pro-

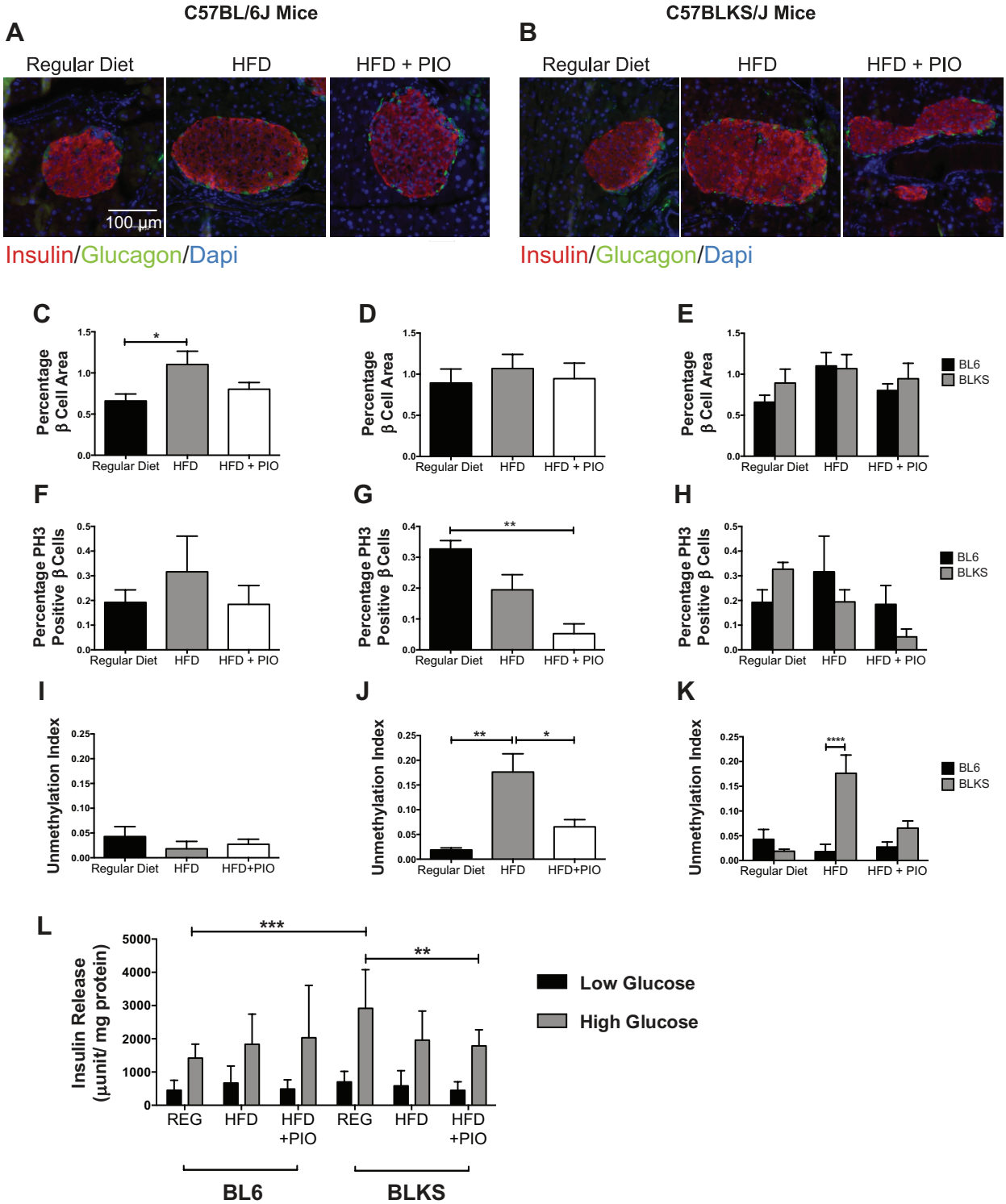

Fig. 5. BL6 mice demonstrate increased β-cell area in response to HFD, whereas BLKS mice show increased β-cell death. *A and B*: immunofluorescent staining of insulin and glucagon was performed on pancreatic sections from BL6 and BLKS mice fed Regular Diet, HFD, or HFD+PIO for 16 wk. *C–E*: β-cell area was quantitated; $n = 5–6$ mice per treatment group. *F–H*: nos. of phosphohistone H3 (PH3)- and insulin-positive cells/total insulin positive cells were quantitated in each group. Scale bars, 100 μm; $n = 3–4$ mice per treatment group. *I–K*: unmethylation index of preproinsulin DNA was calculated as a measure of β-cell death based on RT-PCR of serum after 12–13 wk on diet; $n = 5$ mice per treatment group. *L*: glucose-stimulated insulin secretion (GSIS) was performed in isolated islets from 6 mice in each treatment group. Secreted insulin was normalized to total protein content of islet fraction; $n = 4$ mice per treatment group. Results are displayed as means ± SE. $^*P < 0.05$, $^{**}P < 0.01$, $^{***}P < 0.001$, $^{****}P < 0.0001$ for indicated comparisons.

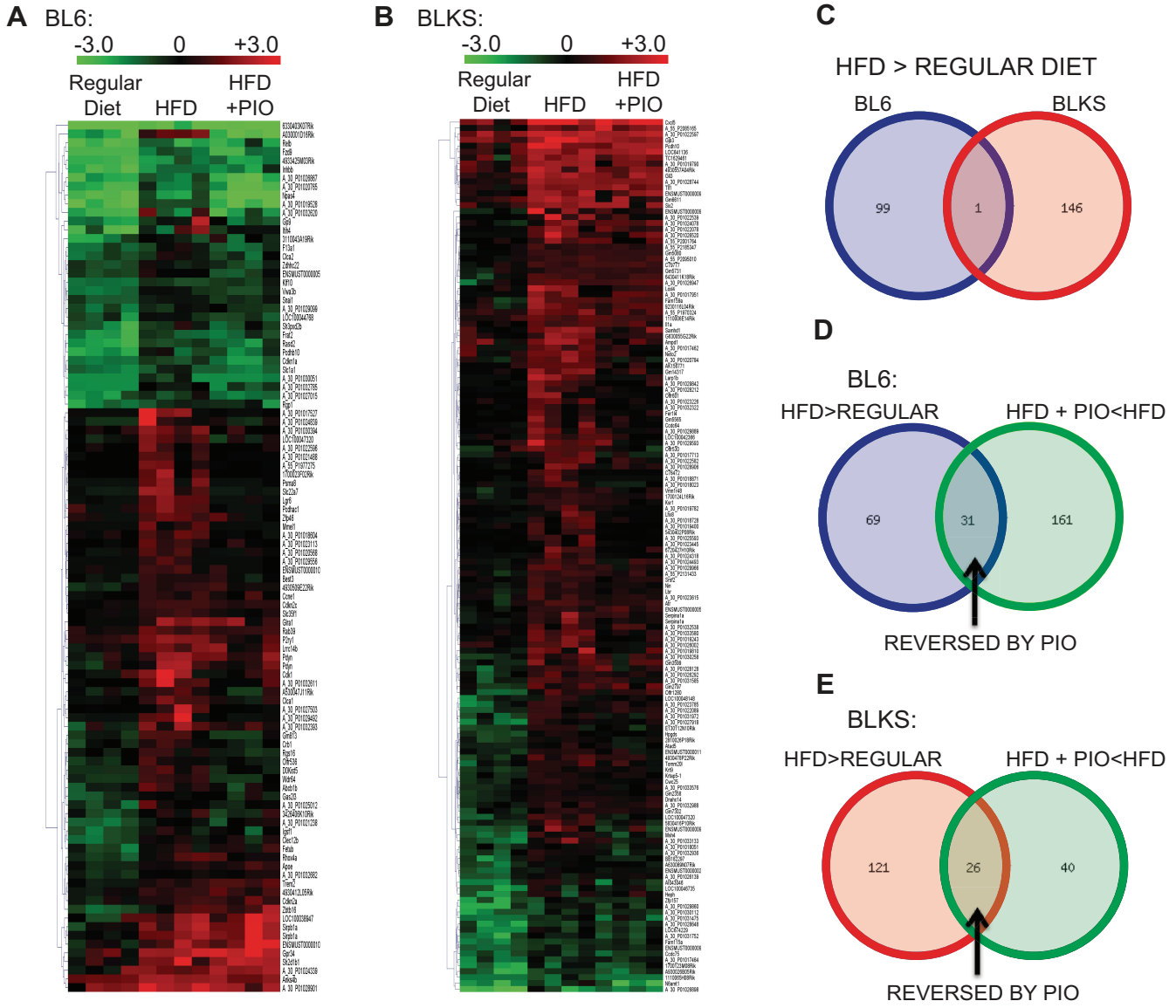

Fig. 6. Islet gene expression upregulated by HFD differs between BL6 and BLKS strains. RNA isolated from islets of BL6 and BLKS mice fed Regular Diet, HFD, or HFD+PIO for 12 wk was analyzed using Agilent Whole Mouse Genome Oligo Microarray. Differential gene expression in BL6 groups (*A*) and BLKS groups (*B*) for genes increased by HFD is depicted using a heat map. Venn diagrams depict overlap in genes (*C*) with increased expression in BL6 and BLKS mice on HFD, and reversal of HFD-induced increases in gene expression with PIO treatment in BL6 (*D*) and BLKS (*E*) mice; n = 4 mice per treatment group.

nounced during the dark cycle, with BLKS mice having higher mean RQ values for regular diet, HFD and HFD+PIO compared with BL6 mice in the same groups (Fig. 10*H*). During the light cycle, only BLKS mice in the HFD+PIO group had a higher RQ than the corresponding BL6 mice (Fig. 10*E*).

Percent relative cumulative frequency (PRCF) curves were generated from 24-h RQ data as previously described to quantitate differences in relative metabolic flexibility or capability to alternate between different fuel substrates as an energy source (Fig. 10, *I–M*) (34). For both strains of mice, the PRCF hill slope significantly increased with HFD (Fig. 10, *K–M*), indicating decreased metabolic flexibility with HFD treatment. Interestingly, PIO further increased the hill slope compared with HFD alone in BL6 mice but did not alter the slope in BLKS mice. BLKS mice tended to have more metabolic flexibility across treatment groups, with a significant difference in slope for animals on HFD and HFD+PIO. Together, these findings suggest that BL6 mice have impaired metabolic flexibility compared with BLKS mice, which is exacerbated by HFD and further worsened by PIO.

BLKS mice have increased calculated EE. Finally, EE was calculated according to the following formula: EE = [3.815 + 1.232 × RQ] × $\dot{V}O_2$ × 0.001 [kcal/(kgxh)]. Total calculated EE decreased in BLKS mice on HFD compared with regular diet but was unchanged between these groups in BL6 mice (Fig. 11, *A, B, D, E*). Interestingly, the addition of PIO to HFD increased EE in both strains, although this difference was more pronounced in BL6 mice (Fig. 11, *A, B, D, E*). BLKS mice on regular diet and HFD alone had significantly greater EE than BL6 mice in corresponding groups throughout the monitoring period (Fig. 11, *C, F*).

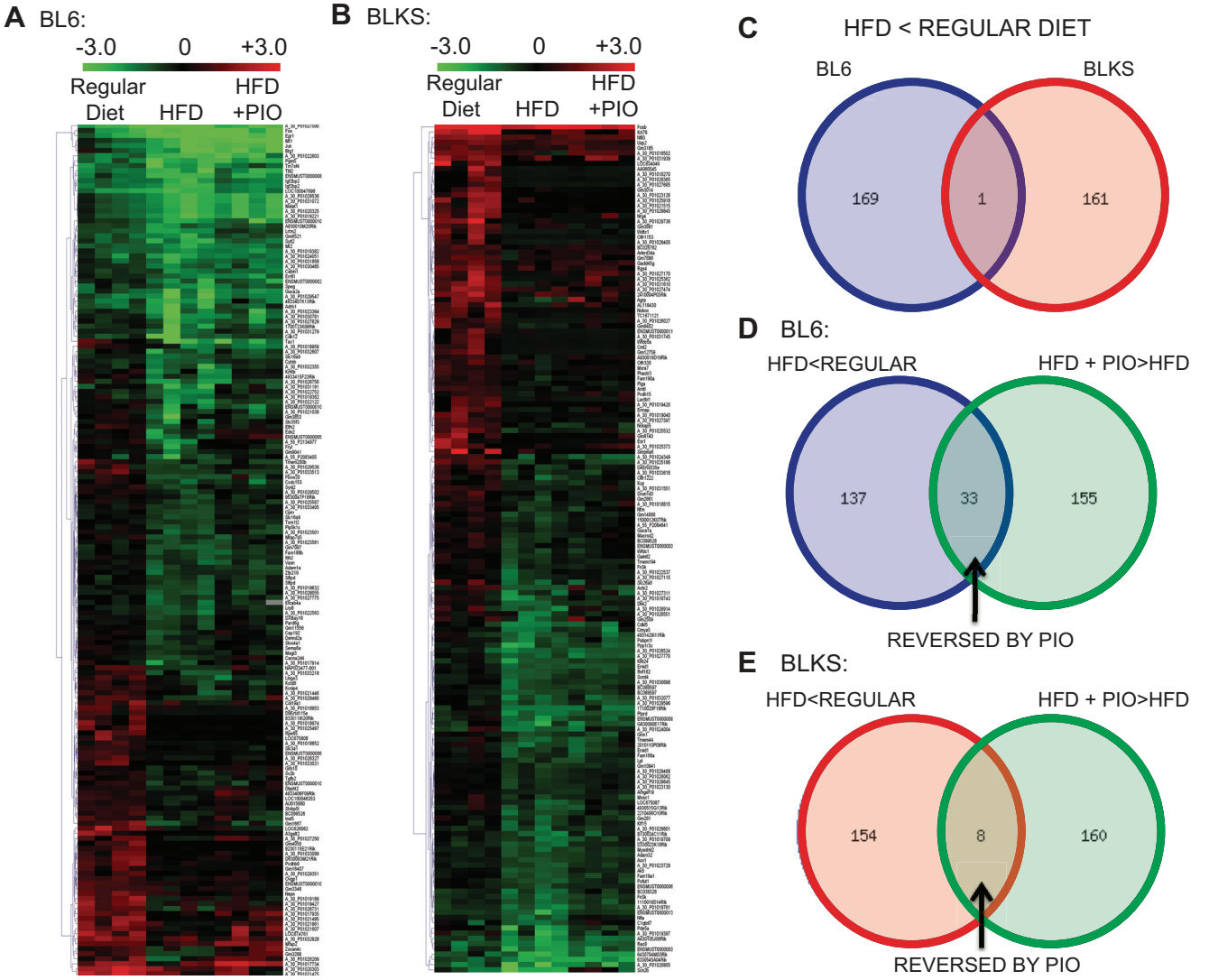

Fig. 7. Islet gene expression decreased by HFD is differentially regulated between BL6 and BLKS strains. RNA isolated from islets of BL6 and BLKS mice fed Regular Diet, HFD, or HFD+PIO for 12 wk was analyzed using Agilent Whole Mouse Genome Oligo Microarray. Differential gene expression in BL6 groups (*A*) and BLKS groups (*B*) for genes decreased by HFD is depicted using a heat map. Venn diagrams depict overlap in genes (*C*) with decreased expression in BL6 and BLKS mice on HFD, and reversal of HFD-induced decreases in gene expression with PIO treatment in BL6 (*D*) and BLKS (*E*) mice; $n = 4$ mice per treatment group.

DISCUSSION

The goal of our study was to define the unique compensatory mechanisms through which BL6 and BLKS mice respond to HFD treatment and to characterize differences in strain responses to PIO treatment initiated concurrently with HFD. While neither strain progressed to frank diabetes during the study, treatment with chow containing 42% of calories from fat led to diet-induced obesity and impaired glucose tolerance and offered an opportunity to phenotype body composition, glucose metabolism, β-cell function and architecture, and energy metabolism in these two commonly used inbred strains of mice.

Analysis of these two particular strains was undertaken for several reasons. First, they are genetically related and share ~70% overlap in their genome. Therefore, phenotypic differences may form the foundation for studies to uncover key modifier genes. Second, the responses of these strains differ significantly in the setting of functional leptin deficiency (*ob/ob* and *db/db* mice), where both strains are polyphagic and initially hyperglycemic. Interestingly, the BL6 mouse is able to compensate with increased insulin production and develops only glucose intolerance, whereas the BLKS strain develops severe and progressive hyperglycemia with islet atrophy (18). In the context of the two parent background strains, the mechanistic reasons for these divergent phenotypes are incompletely understood. Finally, many knockout and transgenic strains are bred congenic on the BL6 strain, and we sought to define how broadly applicable the BL6 response might be to divergent human populations.

Our results show that BL6 mice consumed consistent grams of food but more kilocalories when challenged with HFD. They responded to increased weight and visceral fat accumulation with hyperinsulinemia and hyperleptinemia and had increased visceral fat leptin gene expression and decreased

Table 1. *Differentially expressed genes in BL6 and BLKS islets after 12 wk of HFD*

Gene	Probe	Category	Description
Increased in BL6 mice on HFD			
*Ccne1**	A_51_P408946	Cell cycle/growth/proliferation	Cyclin E1
*Cdkn2a**	A_55_P2008437	Cell cycle/growth/proliferation	Cyclin-dependent kinase inhibitor 2A, transcript variant 1
*Cdkn2c**	A_55_P2074796	Cell cycle/growth/proliferation	Cyclin-dependent kinase inhibitor 2C (p18, inhibits CDK4)
*Gas2l3**	A_55_P2064676	Cell cycle/growth/proliferation	Growth arrest-specific 2 like 3
Cdkn1a#	A_51_P363947	Cell cycle/growth/proliferation	Cyclin-dependent kinase inhibitor 1A (P21), transcript variant 1
Rgs16	A_51_P249286	Cell cycle/growth/proliferation	Regulator of G-protein signaling 16
Sh2d1b1	A_51_P496540	Insulin signaling and growth adaptation	SH2 domain protein 1B1
*Rab39**	A_51_P351217	Member of RAS oncogene family, Membrane trafficking	RAB39, member RAS oncogene family
Decreased in BL6 mice on HFD			
Cdk12#	A_55_P1999187	Cell cycle/growth/proliferation	Cyclin-dependent kinase 12, transcript variant 3
Jun	A_55_P2158990	Cell cycle/growth/proliferation	Jun oncogene
Fosb	A_55_P2113051	Cell cycle/growth/proliferation	FBJ osteosarcoma oncogene B
Igf2bp2#	A_55_P2170737	Cell cycle/growth/proliferation	Insulin-like growth factor 2 mRNA binding protein 2
Grb10	A_55_P1955457	Cell cycle/growth/proliferation	Growth factor receptor bound protein 10
Egr1	A_51_P367866	Cell cycle/growth/proliferation	Early growth response 2
Btg1	A_55_P2181191	Cell cycle/growth/proliferation	B-cell translocation gene 1, anti-proliferative
Errfi1	A_55_P2016105	Cell cycle/growth/proliferation	ERBB receptor feedback inhibitor 1
Tgfb2	A_51_P317640	Inflammation/inflammatory response	Transforming growth factor, beta 2
Cabin1	A_52_P93422	Calcineurin signal transduction	Calcineurin binding protein 1
ENSMUST00000023526	A_55_P2105983	Insulin secretion	Syntaxin binding protein 5-like
Increased in BLKS mice on HFD			
Il1a	A_52_P100926	Inflammation/inflammatory response	Interleukin 1 alpha
CxCl5	A_55_P1990032	Inflammation/inflammatory response	Chemokine (C-X-X motif) ligand 5
Hpgds	A_52_P536796	Inflammation/inflammatory response	Hematopoietic prostaglandin D synthase
Decreased in BLKS mice on HFD			
Gadd45 g	A_51_P315904	Cell cycle/growth/proliferation	Growth arrest and DNA-damage-inducible 45 gamma
Cdk15	A_55_P2043734	Cell cycle/growth/proliferation	Cyclin-dependent kinase-like 5
Nrg4	A_55_P2185905	Cell cycle/growth/proliferation	Neuregulin 4
Nfil3	A_55_P2035320	Inflammation/inflammatory response	Nuclear factor, interleukin 3, regulated

BL6, C57BL6/J; BLKS, C57BLKS/J. *Similar pattern of differential regulation in database comparing *ob/ob* BL6 and BTBR mice. #Reversed by treatment with pioglitazone.

adiponectin expression. In contrast, BLKS mice, which were more insulin sensitive at baseline, responded to the challenge of HFD by restricting food intake and increasing movement, ultimately limiting weight gain and protecting themselves from the same degree of metabolic dysfunction encountered by BL6 mice. Notably absent in the BLKS response was any increase in β-cell area or proliferation or insulin output. To the contrary, BLKS mice on HFD showed a striking increase in serum unmethylated insulin DNA, reflecting β-cell death in response to HFD.

The metabolism field frequently utilizes knockout and transgenic models bred congenic on the BL6 background for analysis. Although the need for consistency in background within a cohort is appreciated in order to adequately interpret experimental findings, our study suggests that variance from the use of a BL6 background strain may be informative in certain situations. For example, certain Asian and Native American populations are predisposed to T2DM at younger ages and lower body mass index (BMI) values compared with Caucasians and manifest more pronounced alterations in β-cell function (4, 6, 23). This susceptibility to glucose intolerance mirrors that of BLKS mice. Asian populations are also predisposed to development of metabolic syndrome at lower BMI values compared with other ethnic backgrounds (28). This predisposition parallels the vulnerability of BLKS mice to visceral fat accumulation on HFD despite decreased intake and overall weight gain. Interestingly, BLKS mice on HFD have previously been noted to have increased development of atherosclerosis compared with BL6 mice (30).

BLKS mice responded to increased chow energy density by limiting intake and increasing activity, mirroring individuals who maintain normal weight despite the modern obesogenic environment. Similar to mice in our study, predisposition to increased activity thermogenesis appears to be largely determined by genetics (19). In lean individuals who are challenged with chronic overfeeding, resistance to obesity was directly predicted by spontaneous increases in activity (25). Conversely, BL6 mice, which consumed significantly more kilocalories per day when offered an energy-dense diet, may provide a more appropriate model for obese individuals with similar maladaptive responses, which are amplified by prolonged exposure to the typical modern environment of excess calories and reduced need for movement (10, 37). Similarly to the BL6 strain, exposure of many humans to this environment translates to increased energy intake and decreased planned and spontaneous activity, ultimately leading to obesity in individuals without any inherent self-regulation to keep the process in check. (17, 26). Given these findings, the BL6 strain would be particularly advantageous when studying genes that might modify the development of feeding behavior or adiposity.

Because GWAS studies point to underlying β-cell susceptibility as the most consistently identified genetic risk factor for T2DM, we carefully analyzed the β-cell phenotype of both

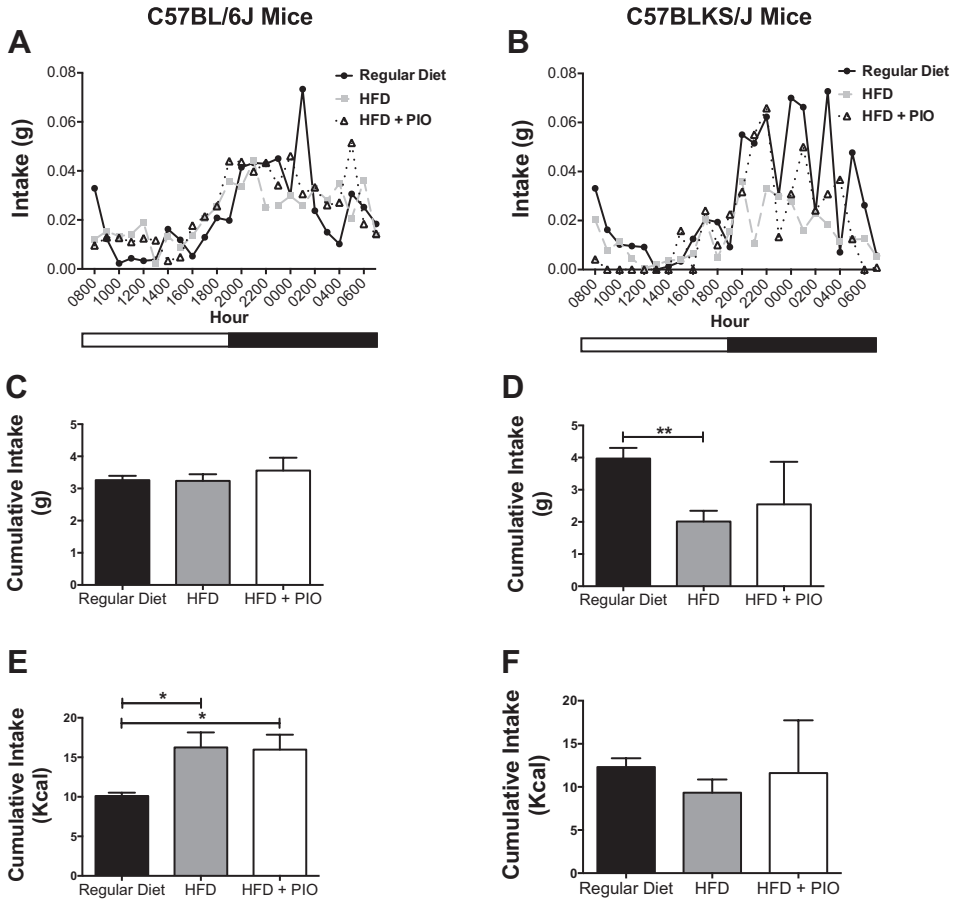

Fig. 8. BLKS mice demonstrate consistent kcal intake on HFD, whereas BL6 mice exhibit significantly increased kcal intake on HFD, and PIO does not affect feeding behavior in BL6 mice. *A* and *B*: 24-h intake (g) during light (0700–1900) and dark cycles (1900–0700) was calculated. *C* and *D*: cumulative intake (g) during monitoring period for BL6 and BLKS mice. *E* and *F*: cumulative kcal intake during monitoring period was calculated. Results are displayed as means ± SE; $n = 6–8$ per treatment group, except BLKS mice on HFD+PIO, where $n = 2$. This group exhibited "shredding" behavior of chow without subsequent consumption, affecting accuracy of measurement. Results are displayed for all groups, but BLKS HFD+PIO mice were subsequently excluded from statistical analysis of intake because shredding behavior required exclusion of a majority of animals studied. Results are displayed as means ± SEM; $n = 8$ per treatment group. $^{*}P < 0.05$, $^{**}P < 0.01$, $^{***}P < 0.001$, $^{****}P < 0.0001$ for indicated comparisons.

strains in response to HFD (13). The absence of major identified defects in β-cell function assessed by GSIS likely reflects our choice of a more moderate HFD (42% of calories from fat). This is in contrast to other studies utilizing diets with 60% of calories from fat, in which abnormalities in GSIS were identified (31, 49). An important and unique compensatory response of the BL6 strain challenged with HFD was to increase β-cell area and proliferation with the parallel development of significant hyperinsulinemia, consistent with previous studies demonstrating the high proliferative capacity of BL6 islets compared with BLKS mice (24, 42). This strain's ability to compensate at the β-cell level is notable, especially given the mutation in the Nnt gene. The Nnt mutation developed in the Jackson Lab C57BL6/J strain and has been reported to affect insulin secretion and may likely contribute to baseline differences in glucose tolerance seen between strains on regular diet (43). However, our findings may also imply a higher threshold for the development of a dysfunctional phenotype for β-cell gene knockout studies performed in the BL6 strain. Interestingly, no increase in serum insulin or the percentage of β-cell area or proliferation was noted in the BLKS cohort. To the contrary, despite less weight gain, BLKS mice on HFD have increased β-cell death and similar worsening in glucose tolerance compared with BL6 mice. This β-cell dysfunction in response to the stress of mild diet-induced obesity and increased visceral fat accumulation recapitulates the decompensation experienced by this strain on the *db/db* and *ob/ob* backgrounds (18). Intriguingly, with an intact leptin signaling system, the BLKS strain is able to compensate for the effects of HFD by limiting weight gain through restoration of energy balance with decreased kilocalorie consumption that is complemented by increased activity. A similar response to leptin signaling appears to be absent in BL6 mice, which continue to generate a positive energy balance on HFD, accumulating larger amounts of body fat, with apparent increased leptin resistance and significantly elevated serum leptin levels. The dependency of the BLKS strain to rely on decreased food intake to maintain metabolic homeostasis may also provide additional insight into why these animals rapidly decompensate when leptin signaling and this "brake" on appetite is impaired in the *db/db* and *ob/ob* backgrounds.

Because of the distinct β-cell phenotype observed between strains, we utilized a microarray to study changes in islet gene expression as a function of background strain and dietary and drug intervention. We found that a variety of genes were differentially expressed between strains and treatment groups. Several genes known to encode proteins that regulate cell cycle and growth were found to be different between BL6 and BLKS mice in response to HFD. A seminal report from the Attie group has previously compared the diabetes-resistant BL6 and diabetes-susceptible BTBR strains with *ob/ob* mutations (21). Genes with similar patterns of expression in diabetes-resistant BL6 *ob/ob* mice and BL6 mice treated with HFD in our study relative to the comparator diabetes-susceptible strain included cyclin E1, cyclin-dependent kinase inhibitor 2a, cyclin-dependent kinase inhibitor 2c, growth arrest specific 2-like 3, and the

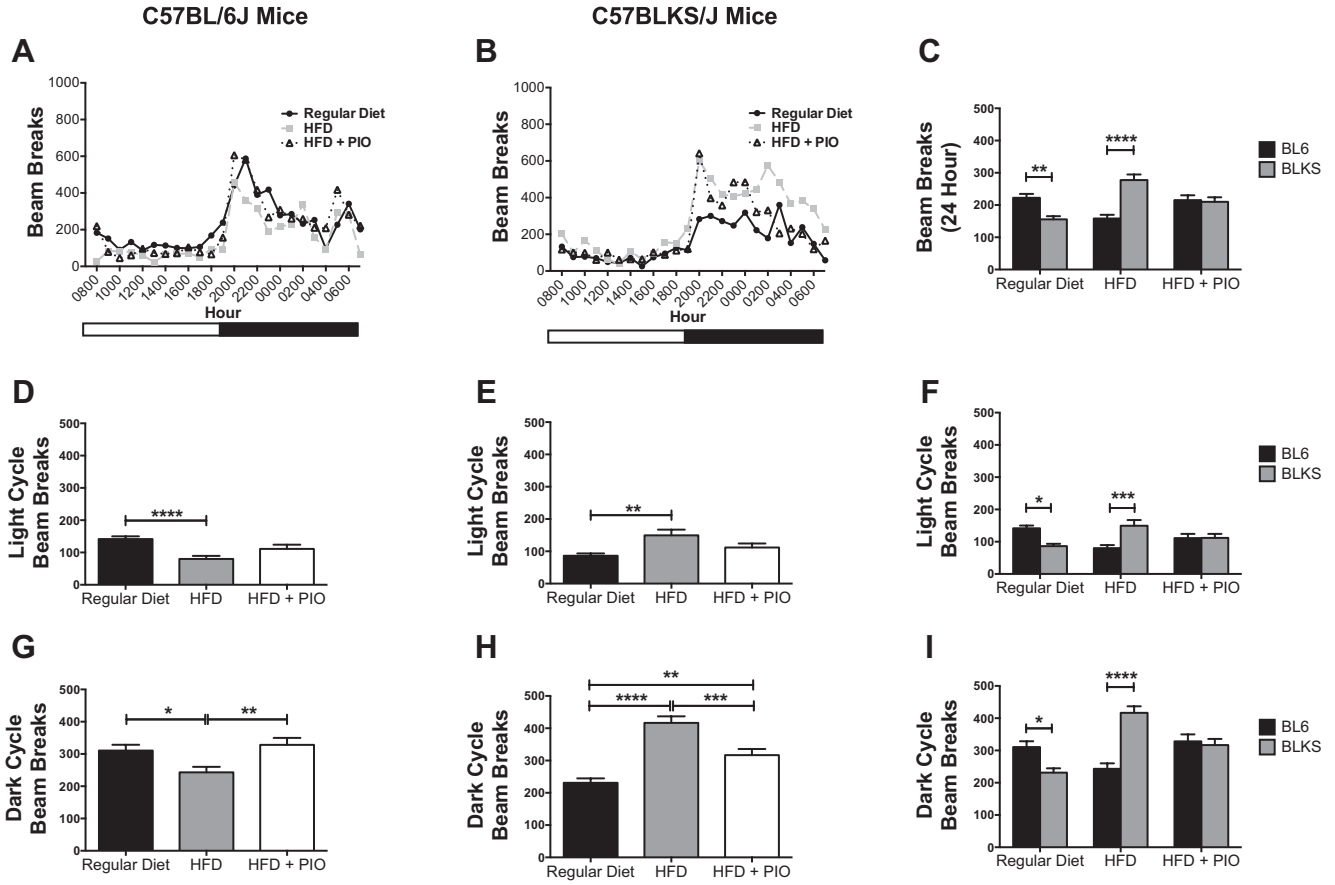

Fig. 9. BLKS mice demonstrate increased movement in response to HFD. BL6 and BLKS mice fed Regular Diet, HFD, or HFD+PIO for 12 wk were singly housed in a PhenoMaster LabMaster indirect calorimeter and activity was assessed by recording the number of beam breaks occurring in the *x*+*y*- and *z*-axes. *A–C*: hourly beam breaks during light (0700–1900) and dark cycles (1900–0700) were recorded over a 24-h period. Average number of beam breaks during light (*D–F*) and dark cycle (*G–I*) in each treatment group. Results are displayed as means ± SE; $n = 8$ per treatment group. *$P < 0.05$, **$P < 0.01$, ***$P < 0.001$, ****$P < 0.0001$ for indicated comparisons.

member of the Ras oncogene family Rab39. Activation of growth-regulating pathways is consistent with changes in β-cell area and proliferation seen in the BL6 strain.

BLKS islets exposed to high glucose ex vivo have been demonstrated to express increased inflammatory response genes (3). Of note, our microarray data showed increased expression of a number of these pro-inflammatory genes in islets from BLKS mice in all treatment groups compared with BL6 animals. Furthermore, expression of several pro-inflammatory genes like IL-1α and CXCL5 increased with HFD. Interestingly, IL-1α and CXCL5 have previously been linked to hyperglycemia and diabetes susceptibility in humans (16, 27). These changes suggest a hyperactive inflammatory response pathway and could explain, at least in part, the β-cell dysfunction in BLKS animals treated with HFD.

In aggregate, our microarray data suggest that differences in islet gene expression may contribute to important aspects of the phenotypic differences observed between the BL6 and BLKS strains. It is noteworthy that, despite 70% homology, gene expression changes in response to HFD with or without PIO were quite distinct between the two strains, with virtually no overlap in gene expression profiles noted between strains. The relevance of changes observed in BL6 and BLKS islets will need to be more fully explored in future studies. For example, it is interesting to note that nearly equal numbers of positive and negative regulators of the cell cycle are represented in BL6 islets from HFD-treated mice, clearly suggesting the need for studies that investigate changes in protein expression and posttranslational modification as well as alterations in nuclear and cytoplasmic localization for cell proteins that regulate growth and proliferation. However, here we provide the full microarray data for additional hypothesis generation and to serve as a resource to the community.

BL6 and BLKS mice fed HFD also exhibited distinct responses to PPARγ agonist therapy. Notably, islet microarray revealed that PIO treatment reversed changes in gene expression in 24% of differentially regulated genes in BL6 mice on HFD vs. 11% of differentially regulated genes in BLKS mice on HFD. The decrease in reversal of HFD-induced gene expression in BLKS islets could be related to decreased weight gain and insulin resistance in this group, which could limit affected genes that could be improved by treatment with PIO. However, similar numbers of genes were differentially expressed in islets of BL6 and BLKS mice on HFD, which would suggest that the decreased response of BLKS islets reflects a decreased sensitivity to the drug's effects.

Phenotypic differences in the response to PIO were also noted. Treatment with PIO improved glucose tolerance and decreased visceral fat as a percentage of total weight in BL6 mice but had no effect on visceral fat in BLKS mice. BLKS

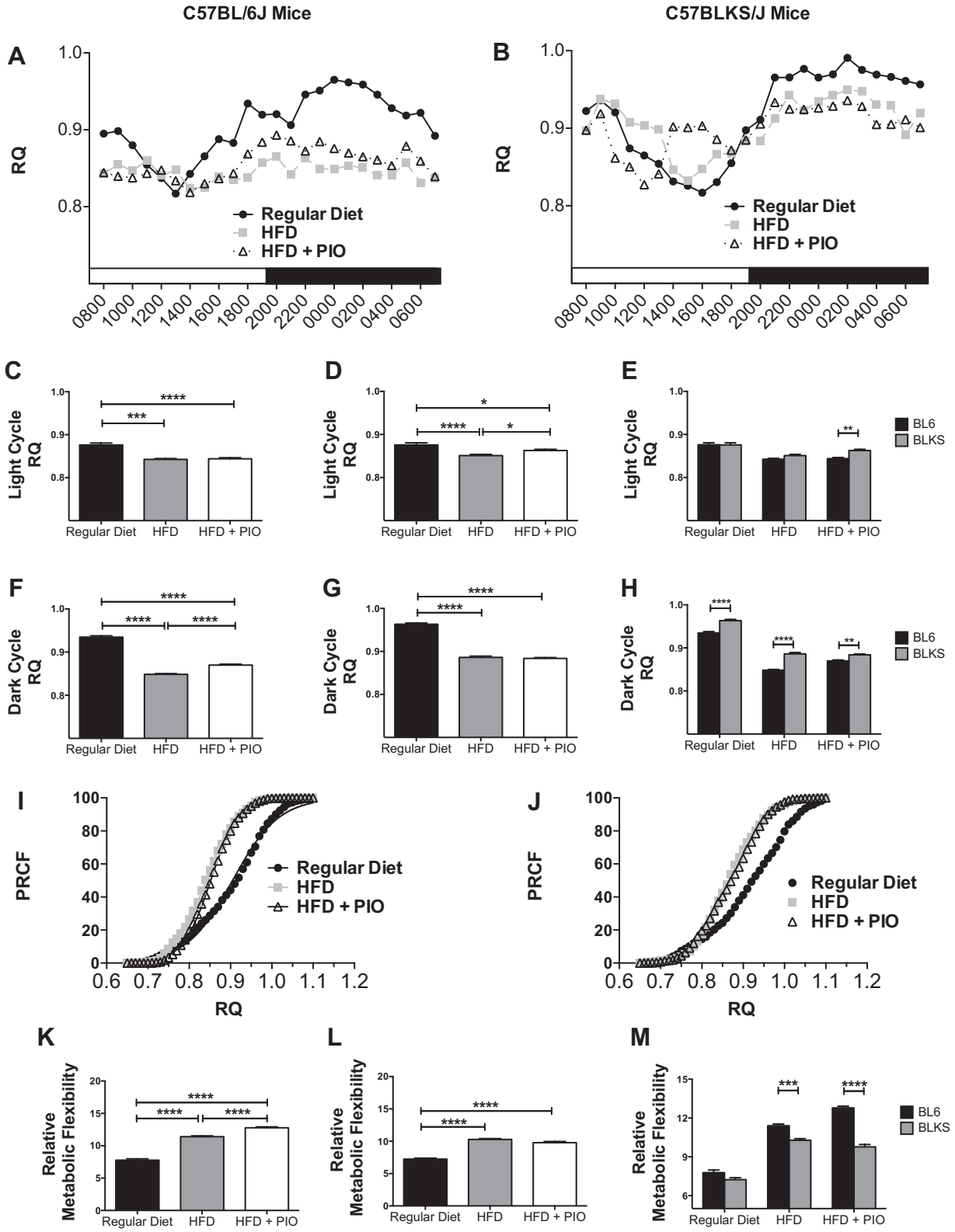

Fig. 10. BLKS mice demonstrate increased respiratory quotient (RQ) values. BL6 and BLKS mice fed Regular Diet, HFD, or HFD+PIO for 12 wk were singly housed in a PhenoMaster LabMaster indirect calorimeter and RQs were calculated. *A* and *B*: hourly RQ values during light (0700–1900) and dark cycles (1900–0700) were obtained over a 24-h period. *C–E*: average RQ values during the light cycle were calculated. *F–H*: average RQ values during the dark cycle. *I–J*: percent relative cumulative frequency (PRCF) curves were generated using RQ values over a 24-h period. *K–M*: Hill slopes of PRCF curves were compared as a measure of metabolic flexibility. Results are displayed as means ± SE; $n = 8$ per treatment group. *$P < 0.05$, **$P < 0.01$, ***$P < 0.001$, ****$P < 0.0001$ for indicated comparisons.

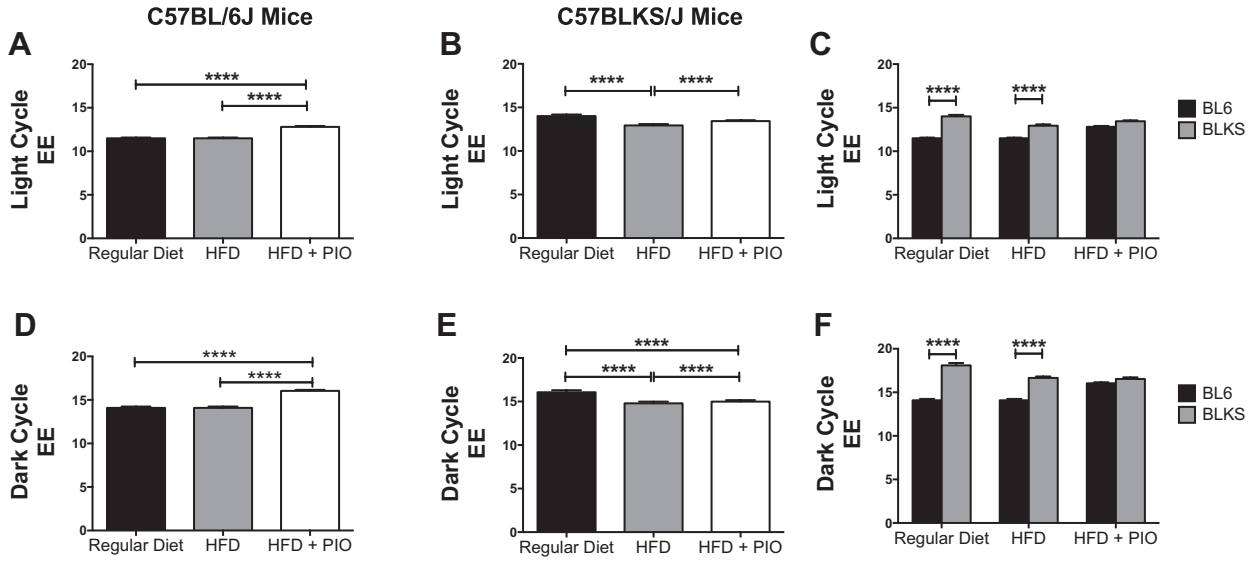

Fig. 11. Calculated energy expenditure (EE) is decreased in BLKS mice on HFD and increased in response to HFD+PIO in both strains. BLKS mice have significantly higher levels of EE than BL6 mice. BL6 and BLKS mice fed Regular Diet, HFD, or HFD+PIO for 12 wk were singly housed in a PhenoMaster LabMaster indirect calorimeter, and EE was calculated. *A–C*: hourly EE normalized to lean mass during light (0700–1900) and dark cycles (1900–0700) was calculated over a 24-h period. Average EE values during light cycle (*D–F*) and dark cycle (*G–I*). Results are displayed as means ± SE; $n = 4$ per treatment group. $^{*}P < 0.05$, $^{**}P < 0.01$, $^{***}P < 0.001$, $^{****}P < 0.0001$ for indicated comparisons.

mice on PIO had an increase in total body weight, whereas BL6 mice had stable body weight. In BL6 mice, the addition of PIO increased the RQ, with a steeper PRCF curve reflecting decreased metabolic flexibility (33). PIO treatment also increased EE in both strains studied. In contrast, a single dose of PIO has previously been reported to decrease EE acutely in rats; however, no changes in RQ values or locomotor activity were seen between treated and control animals (22). Our results could have been affected by differences in activity seen in HFD+PIO mice. Alternatively, the increase in RQ and EE and worsened metabolic flexibility may represent effects of chronic PIO administration or unique responses of these strains to PIO. The improved metabolic flexibility noted in BLKS mice could be a result of enhanced mitochondrial function, as differences in expression of uncoupling proteins and Nnt have been previously reported between these strains (3, 41).

Activation of hypothalamic PPARγ is known to increase food intake in rats, resulting in a positive energy balance, and to contribute to weight gain caused by treatment with the PPARγ agonist rosiglitazone (35). Interestingly, BL6 mice in our study did not increase food consumption on PIO, suggesting this response may also be affected by genetic background or may alternatively differ between TZD drugs. Consumption of BLKS mice on HFD+PIO was difficult to interpret, because this group was excluded from analysis due to shredding behavior, which did not allow us to accurately calculate food intake in this one group. Nevertheless, differing metabolic responses to PIO between our strains and between published studies in rats likely reflect variations in the range of effects of PPARγ agonists existing between groups of humans, with 30–40% of participants in large-scale clinical trials demonstrating heterogeneity or lack of response to effects of TZDs (9, 47). Notably, human genetic variations in the sequence of the PPARγ locus have been associated with response to TZD treatment (50).

In conclusion, evaluation of the compensatory responses of BL6 and BLKS mouse strains to diet-induced obesity and PPARγ agonist treatment initiated concurrently with HFD revealed important physiological and phenotypic differences. Such variations should be taken into account when designing studies utilizing either of these two models as representative human responses to an obesogenic environment, compensation to HFD, or pharmacological therapies. Finally, our analysis also suggests that strains other than BL6 may have particular utility when extrapolating results to a specific human population or when investigating a specific component of diabetes pathophysiology. Differences in effects of PIO on islet gene expression between strains are especially notable given the expanding field of diabetes pharmacogenomics and known differences in response to TZDs between human populations.

GRANTS

This work was supported by National Institutes of Health Grants T32 DK-065549 (to E. K. Sims), F32 DK-091976 (to D. L. Morris), T32 HL-079995 (to T. Kono), and DCC Pilot and Feasibility Award, K08 DK-080225, R03 DK-089147, R01 DK-093954 (to C. Evans-Molina), R01 DK-60583, and R01 DK-80583 (both to R. G. Mirmira), a Clarian/Indiana University Health Values Research Award, and VA Merit Award 1I01BX001733 (both to C. Evans-Molina).

DISCLOSURES

No conflicts of interest, financial or otherwise, are declared by the author(s).

AUTHOR CONTRIBUTIONS

Author contributions: E.K.S., M.H., D.L.M., S.A.T., T.K., R.G.M., and C.E.-M. conception and design of research; E.K.S., M.H., D.L.M., S.A.T., T.K., Z.Z.C., K.H.D., D.R.M., and N.D.S. performed experiments; E.K.S., S.A.T., and C.E.-M. analyzed data; E.K.S., D.L.M., S.A.T., R.G.M., and C.E.-M. interpreted results of experiments; E.K.S. prepared figures; E.K.S. and C.E.-M. drafted manuscript; E.K.S., M.H., D.L.M., S.A.T., T.K., Z.Z.C., K.H.D., D.R.M., N.D.S., R.G.M., and C.E.-M. edited and revised manuscript; E.K.S., M.H., D.L.M., S.A.T., T.K., Z.Z.C., K.H.D., D.R.M., N.D.S., R.G.M., and C.E.-M. approved final version of manuscript.

REFERENCES

1. **JAX®.** Mice database jaxmice. *jax* .org/strain/000664.html. 9/27/12.
2. **Ackermann Misfeldt A, Costa RH, Gannon M.** Beta-cell proliferation, but not neogenesis, following 60% partial pancreatectomy is impaired in the absence of FoxM1. *Diabetes* 57: 3069–3077, 2008.
3. **Anderson AA, Helmering J, Juan T, Li CM, McCormick J, Graham M, Baker DM, Damore MA, Veniant MM, Lloyd DJ.** Pancreatic islet expression profiling in diabetes-prone C57BLKS/J mice reveals transcriptional differences contributed by DBA loci, including Plagl1 and Nnt. *Pathogenetics* 2: 1, 2009.
4. **Bennett PH, Burch TA, Miller M.** Diabetes mellitus in American (Pima) Indians. *Lancet* 2: 125–128, 1971.
5. **Black BL, Croom J, Eisen EJ, Petro AE, Edwards CL, Surwit RS.** Differential effects of fat and sucrose on body composition in A/J and C57BL/6 mice. *Metab Clin Exper* 47: 1354–1359, 1998.
6. **Chan JC, Malik V, Jia W, Kadowaki T, Yajnik CS, Yoon KH, Hu FB.** Diabetes in Asia: epidemiology, risk factors, and pathophysiology. *JAMA* 301: 2129–2140, 2009.
7. **Collins S, Martin TL, Surwit RS, Robidoux J.** Genetic vulnerability to diet-induced obesity in the C57BL/6J mouse: physiological and molecular characteristics. *Physiol Behav* 81: 243–248, 2004.
8. **Davis RC, Schadt EE, Cervino AC, Peterfy M, Lusis AJ.** Ultrafine mapping of SNPs from mouse strains C57BL/6J, DBA/2J, and C57BLKS/J for loci contributing to diabetes and atherosclerosis susceptibility. *Diabetes* 54: 1191–1199, 2005.
9. **Distefano JK, Watanabe RM.** Pharmacogenetics of anti-diabetes drugs. *Pharmaceuticals (Basel)* 3: 2610–2646, 2010.
10. **Ebbeling CB, Sinclair KB, Pereira MA, Garcia-Lago E, Feldman HA, Ludwig DS.** Compensation for energy intake from fast food among overweight and lean adolescents. *JAMA* 291: 2828–2833, 2004.
11. **Edgar R, Domrachev M, Lash AE.** Gene Expression Omnibus: NCBI gene expression and hybridization array data repository. *Nucleic Acids Res* 30: 207–210, 2002.
12. **Fisher MM, Perez Chumbiauca CN, Mather KJ, Mirmira RG, Tersey SA.** Detection of islet beta cell death in vivo by multiplex PCR analysis of differentially methylated DNA. *Endocrinology* 154: 3476–3481, 2013.
13. **Florez JC.** Newly identified loci highlight beta cell dysfunction as a key cause of type 2 diabetes: where are the insulin resistance genes? *Diabetologia* 51: 1100–1110, 2008.
14. **Francis J, Chakrabarti SK, Garmey JC, Mirmira RG.** Pdx-1 links histone H3-Lys-4 methylation to RNA polymerase II elongation during activation of insulin transcription. *J Biol Chem* 280: 36244–36253, 2005.
15. **Fueger PT, Hernandez AM, Chen YC, Colvin ES.** Assessing replication and beta cell function in adenovirally-transduced isolated rodent islets. *J Vis Exp* Jun 25;(64), 2012.
16. **Hasani Ranjbar S, Amiri P, Zineh I, Langaee TY, Namakchian M, Heshmet R, Sajadi M, Mirzaee M, Rezazadeh E, Balaei P, Tavakkoly Bazzaz J, Gonzalez-Gay MA, Larijani B, Amoli MM.** CXCL5 gene polymorphism association with diabetes mellitus. *Mol Diagn Ther* 12: 391–394, 2008.
17. **Heber D.** An integrative view of obesity. *Am J Clin Nutr* 91: 280S–283S, 2010.
18. **Hummel KP, Coleman DL, Lane PW.** The influence of genetic background on expression of mutations at the diabetes locus in the mouse. I. C57BL-KsJ and C57BL-6J strains. *Biochem Genet* 7: 1–13, 1972.
19. **Johannsen DL, Ravussin E.** Spontaneous physical activity: relationship between fidgeting and body weight control. *Curr Opin Endocrinol Diabetes Obes* 15: 409–415, 2008.
20. **Juan G, Traganos F, James WM, Ray JM, Roberge M, Sauve DM, Anderson H, Darzynkiewicz Z.** Histone H3 phosphorylation and expression of cyclins A and B1 measured in individual cells during their progression through G2 and mitosis. *Cytometry* 32: 71–77, 1998.
21. **Keller MP, Choi Y, Wang P, Davis DB, Rabaglia ME, Oler AT, Stapleton DS, Argmann C, Schueler KL, Edwards S, Steinberg HA, Chaibub Neto E, Kleinhanz R, Turner S, Hellerstein MK, Schadt EE, Yandell BS, Kendziorski C, Attie AD.** A gene expression network model of type 2 diabetes links cell cycle regulation in islets with diabetes susceptibility. *Genome Res* 18: 706–716, 2008.
22. **Lamontagne J, Jalbert-Arsenault E, Pepin E, Peyot ML, Ruderman NB, Nolan CJ, Joly E, Madiraju SR, Poitout V, Prentki M.** Pioglitazone acutely reduces energy metabolism and insulin secretion in rats. *Diabetes* 62: 2122–2129, 2013.
23. **Lee JW, Brancati FL, Yeh HC.** Trends in the prevalence of type 2 diabetes in Asians versus whites: results from the United States National Health Interview Survey, 1997–2008. *Diabetes Care* 34: 353–357, 2011.
24. **Leiter EH.** Analysis of differential survival of syngeneic islets transplanted into hyperglycemic C57BL/6J versus C57BL/KsJ mice. *Transplantation* 44: 401–406, 1987.
25. **Levine JA, Eberhardt NL, Jensen MD.** Role of nonexercise activity thermogenesis in resistance to fat gain in humans. *Science* 283: 212–214, 1999.
26. **Lowe MR.** Self-regulation of energy intake in the prevention and treatment of obesity: is it feasible? *Obes* Res 11 *Suppl*: 44S–59S, 2003.
27. **Luotola K, Paakkonen R, Alanne M, Lanki T, Moilanen L, Surakka I, Pietila A, Kahonen M, Nieminen MS, Kesaniemi YA, Peters A, Jula A, Perola M, Salomaa V.** Association of variation in the interleukin-1 gene family with diabetes and glucose homeostasis. *J Clin Endocrinol Metab* 94: 4575–4583, 2009.
28. **Misra A, Khurana L.** The metabolic syndrome in South Asians: epidemiology, determinants, and prevention. *Metab Synd Relat Dis* 7: 497–514, 2009.
29. **Naggert JK, Mu JL, Frankel W, Bailey DW, Paigen B.** Genomic analysis of the C57BL/Ks mouse strain. *Mamm Genome* 6: 131–133, 1995.
30. **Nishina PM, Naggert JK, Verstuyft J, Paigen B.** Atherosclerosis in genetically obese mice: the mutants obese, diabetes, fat, tubby, and lethal yellow. *Metabolism* 43: 554–558, 1994.
31. **Petro AE, Cotter J, Cooper DA, Peters JC, Surwit SJ, Surwit RS.** Fat, carbohydrate, and calories in the development of diabetes and obesity in the C57BL/6J mouse. *Metab Clin Exper* 53: 454–457, 2004.
32. **Peyot ML, Pepin E, Lamontagne J, Latour MG, Zarrouki B, Lussier R, Pineda M, Jetton TL, Madiraju SR, Joly E, Prentki M.** Beta-cell failure in diet-induced obese mice stratified according to body weight gain: secretory dysfunction and altered islet lipid metabolism without steatosis or reduced beta-cell mass. *Diabetes* 59: 2178–2187, 2010.
33. **Riachi M, Himms-Hagen J, Harper ME.** Percent relative cumulative frequency analysis in indirect calorimetry: application to studies of transgenic mice. *Can J Physiol Pharmacol* 82: 1075–1083, 2004.
34. **Riachi M, Himms-Hagen J, Harper ME.** Percent relative cumulative frequency analysis in indirect calorimetry: application to studies of transgenic mice. *Can J Physiol Pharmacol* 82: 1075–1083, 2004.
35. **Ryan KK, Li B, Grayson BE, Matter EK, Woods SC, Seeley RJ.** A role for central nervous system PPAR-gamma in the regulation of energy balance. *Nat Med* 17: 623–626, 2011.
36. **Schneider CA, Rasband WS, Eliceiri KW.** NIH Image to ImageJ: 25 years of image analysis. *Nat Methods* 9: 671–675, 2012.
37. **Speechly DP, Buffenstein R.** Appetite dysfunction in obese males: evidence for role of hyperinsulinaemia in passive overconsumption with a high fat diet. *Eur J Clin Nutr* 54: 225–233, 2000.
38. **Stull ND, Breite A, McCarthy R, Tersey SA, Mirmira RG.** Mouse islet of Langerhans isolation using a combination of purified collagenase and neutral protease. *J Vis Exp* Sep 7;(67), 2012.
39. **Surwit R, Seldin M, Kuhn CM, Secor C, Feinglos M.** Diet-induced obesity and diabetes in C57BL/6J and C57 BL/KsJ mice. *Mouse Genome* 92: 523–525, 1994.
40. **Surwit RS, Kuhn CM, Cochrane C, McCubbin JA, Feinglos MN.** Diet-induced type II diabetes in C57BL/6J mice. *Diabetes* 37: 1163–1167, 1988.
41. **Surwit RS, Wang S, Petro AE, Sanchis D, Raimbault S, Ricquier D, Collins S.** Diet-induced changes in uncoupling proteins in obesity-prone and obesity-resistant strains of mice. *Proc Natl Acad Sci USA* 95: 4061–4065, 1998.
42. **Swenne I, Andersson A.** Effect of genetic background on the capacity for islet cell replication in mice. *Diabetologia* 27: 464–467, 1984.
43. **Toye AA, Lippiat JD, Proks P, Shimomura K, Bentley L, Hugill A, Mijat V, Goldsworthy M, Moir L, Haynes A, Quarterman J, Freeman HC, Ashcroft FM, Cox RD.** A genetic and physiological study of impaired glucose homeostasis control in C57BL/6J mice. *Diabetologia* 48: 675–686, 2005.
44. **Tschop M, Statnick MA, Suter TM, Heiman ML.** GH-releasing peptide-2 increases fat mass in mice lacking NPY: indication for a crucial mediating role of hypothalamic agouti-related protein. *Endocrinology* 143: 558–568, 2002.
45. **Turner RC, Cull CA, Frighi V, Holman RR.** Glycemic control with diet, sulfonylurea, metformin, or insulin in patients with type 2 diabetes mellitus: progressive requirement for multiple therapies (UKPDS 49). UK Prospective Diabetes Study (UKPDS) Group. *JAMA* 281: 2005–2012, 1999.
46. **Wallace TM, Levy JC, Matthews DR.** Use and abuse of HOMA modeling. *Diabetes Care* 27: 1487–1495, 2004.

47. **Watanabe RM.** Drugs, diabetes and pharmacogenomics: the road to personalized therapy. *Pharmacogenomics* 12: 699–701, 2011.
48. **Wheeler E, Barroso I.** Genome-wide association studies and type 2 diabetes. *Brief Funct Genomics* 10: 52–60, 2011.
49. **Winzell MS, Ahren B.** The high-fat diet-fed mouse: a model for studying mechanisms and treatment of impaired glucose tolerance and type 2 diabetes. *Diabetes* 53, *Suppl* 3: S215–S219, 2004.
50. **Wolford JK, Yeatts KA, Dhanjal SK, Black MH, Xiang AH, Buchanan TA, Watanabe RM.** Sequence variation in PPARG may underlie differential response to troglitazone. *Diabetes* 54: 3319–3325, 2005.
51. **Zeitler P, Hirst K, Pyle L, Linder B, Copeland K, Arslanian S, Cuttler L, Nathan DM, Tollefsen S, Wilfley D, Kaufman F.** A clinical trial to maintain glycemic control in youth with type 2 diabetes. *N Engl J Med* 366: 2247–2256, 2012.